# Effects of Cooling Rate and Physical Aging on the Gas Transport Properties in Polycarbonate

**Christelle M. Laot,‡ Eva Marand,* B. Schmittmann,† and R. K. P. Zia†**

*Department of Chemical Engineering, Virginia Polytechnic Institute and State University, Blacksburg, Virginia 24061-0211*

*Received November 27, 2002*

ABSTRACT: The gas transport properties of bisphenol A polycarbonate films were examined as a function of the cooling rate during film processing and subsequent physical aging. Interpretation of the permeation properties using results from dynamic mechanical analysis and density measurements indicated that the diffusion coefficient of small gas molecules in glassy polycarbonate is influenced more by the local chain dynamics rather than by the overall free volume content. A one-dimensional lattice model was developed to help probe the effects of the distribution of energy barriers associated with polymer motion on the transport properties. Fast cooling rates generated highly restricted conformations, which hindered local motions leading to increases in the measured activation energy of diffusion. These results correlated well with a lattice model having a broad distribution of energy barriers. Annealing reduced the measured diffusion coefficients, which was shown to be consistent with narrowing of the energy barrier distribution, as well as an increase in the mean barrier energy. Interestingly, the decrease in the diffusion coefficient with aging was found to occur much more slowly in fast-cooled samples, despite the higher initial free volume content. By contrast, properties such as density or isothermal dynamic mechanical properties were more consistent with the free volume model.

## Introduction

Permeation of small molecules through glassy polymeric membranes is believed to occur via the "solution-diffusion" mechanism, consisting of dissolution of the penetrant in the polymer matrix, followed by diffusion across the polymer membrane, and finally desorption of the penetrant. Thus, the transport behavior of gases in polymers is typically characterized by parameters, such a permeability, $P$, diffusivity, $D$, and solubility, $S$, which are related under certain simplifying assumptions by $P = DS$.[1] The gas solubility coefficient is a thermodynamic parameter, which generally increases with increasing gas condensability, the interactions between the gas and the polymer, and free volume in the polymer matrix. Solubility in glassy polymers is typically modeled by simple Henry's law or by the dual sorption model,[2] which takes into account the additional Langmuir-type sorption in the excess free volume voids. The penetrant diffusion coefficient through glassy polymers on the other hand is a kinetic parameter, which is believed to depend on the molecular dynamics of the polymer chains as well as on the overall free volume content. Similar to the Doolittle equation used for the viscosity of polymers above $T_g$,[3,4] the Cohen−Turnbull model[5] suggests a simplified exponential relationship, which relates the diffusion coefficient to the fractional free volume. This relationship appears to correlate diffusion coefficients with free volume fairly well across a wide range of polymer structures.[6−23] However, such correlations tend to compare glassy polymers strictly on the basis of free volume, ignoring any variations in the glass transition temperature or polymer chain flexibility. On the other hand, there are no existing theoretical models, which relate polymer chain dynamics to diffusion. This is because it is difficult to establish which segmental motions actually facilitate diffusion and the appropriate variables that can quantify such motions.

Physical aging of glassy polymers is a nonequilibrium process, which leads to changes in polymer macroscopic properties, such as embrittlement and densification. Several reviews address this topic in the literature.[24−35] The most popular theories describe physical aging in terms of free volume concepts. Free volume can be visualized as dynamic angstrom-sized voids, cavities, or holes, with a distribution of sizes and shapes, dispersed inside the polymeric matrix. According to Struik,[24] physical aging involves relaxation of the nonequilibrium glass via slow self-retarding reorganization of polymer chains toward a thermodynamic equilibrium. This is accomplished by very slow molecular reptation or cooperative motions, leading to long-range dimensional changes. As the amorphous glassy polymer approaches its equilibrium state, the mobility of the short molecular chain segments decreases due to the reduction in free volume.[24] However, not all relaxation changes such as those observed in enthalpy and viscoelastic properties can be directly correlated to changes in free volume. In fact, different properties exhibit different sensitivity and relaxation rates during physical aging.[27,36−38] Thus, in fact, no single uniform model exists that relates the molecular processes occurring to the observed physical changes.

If the gas transport properties, indeed, depend strictly on the overall free volume content as suggested by the Cohen−Turnbull model, we should be able to measure corresponding changes in the diffusion and solubility coefficients upon aging of a glassy polymer. In fact, to date, most effects of physical aging on the gas transport properties in glassy polymers have been explained in terms of free volume changes.[39−47] While decreases in gas sorption are consistent with decreasing free volume,

† Center for Stochastic Processes in Science and Engineering, and Department of Physics, Virginia Polytechnic Institute and State University, Blacksburg, VA.

‡ Current address: Bayer AG, D-51368 Leverkusen, Germany.

* To whom correspondence should be addressed.

10.1021/ma021720o CCC: $25.00 
Published on Web 10/23/2003

there are discrepancies when attributing changes in diffusion coefficients to free volume effects.[48] Since diffusion is a dynamic process, it is more appropriate to correlate changes in gas transport properties upon physical aging with relaxational processes occurring in the polymer matrix. Molecular modeling theories treat diffusion as a thermally activated process, facilitated by localized motions of polymer segments, which temporarily permit the opening of narrow constrictions separating elements of free volume.[49] These energy barriers are lower in flexible polymers because flexible segments can more easily rearrange themselves to accommodate the penetrant molecule. One would also intuitively expect that the distribution of the potential barriers to gas hopping would be related to the distribution of the relaxation times taking place in the polymer matrix. If these relaxation times increase with physical aging, this should in turn decrease the diffusion rate of the penetrant. Ultimately, it would be important to establish how the time scale of the structural relaxations responsible for physical aging correlates with the time scale of the molecular motions, which enable diffusion.

In this work, we examine the relative importance of molecular relaxations and free volume on the gas transport properties in glassy bisphenol A polycarbonate (BPA-PC). In particular, we study the effects of cooling rate from the rubbery state to the glassy state and of subsequent physical aging on the gas transport properties of small gases in BPA-PC. The rate of cooling determines the proximity of the polymer system to the thermodynamic equilibrium. For example, samples that have been quenched possess a higher free volume and a lower, yet wider, distribution of relaxation times compared to samples that have been cooled very slowly. One would expect that, according to well-established theories,[24] subsequent isothermal physical aging of these samples will also proceed at different rates, *being enhanced in rapidly quenched samples, which have more free volume.*

The physical aging of polycarbonate has been studied extensively using a variety of methods, including infrared and NMR spectroscopies and various viscoelastic and thermal techniques.[38,40,50−68] For example, investigations by FTIR spectroscopy of conformational changes occurring in BPA-PC during physical aging below $T_g$[65,66] show shifts from trans−cis to more stable trans−trans conformations with aging time. Since the trans−trans conformations allow closer local packing of the polymer chains than the trans−cis conformations, the results suggest that sub-$T_g$ annealing will lead to closer interchain packing and possibly restricted segmental motions. Pekarski and co-workers[48] have examined the effect of aging and conditioning by $CO_2$ on sorption and diffusion in BPA-PC. Interestingly, they have found that the activation energy for gas diffusion in a conditioned "open" polymer matrix is higher than that measured in aged samples. This result contradicts the predictions of the free volume theory, which states that diffusion should be faster in materials with more free volume. Pekarski et al.[48] explained this result in terms of elastic energy effects induced by the occupation of sorption sites by gas molecules. Although, we believe that conditioning by $CO_2$ expands the matrix and changes the relaxation dynamics of the polymer chains. Such expansion could lower the conformational entropy, decreasing the amplitude and number of permissible local molecular motions and consequently decreasing the diffusion coefficients. Simultaneously, conditioning by $CO_2$ increases the sorption capacity of the polymer matrix, as would be expected if the free volume increases. This has been well documented by Pekarski and other investigations in similar sorption studies of polycarbonate.[48,69−74] In this paper we strive to probe the various changes in the gas transport properties of small gases in polycarbonate subjected to controlled cooling and annealing treatments.

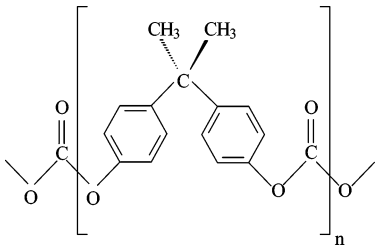


**Figure 1.** Chemical structure of bisphenol A polycarbonate.

## Experimental Details

**Materials.** Bisphenol A polycarbonate (BPA-PC) pellets having a weight-average molecular weight $M_w$ of 34 000 g/mol were purchased from Aldrich Chemical Co. The polydispersity index was found to be approximately 2.2. The chemical structure of BPA-PC is given in Figure 1. Amorphous polymer films were compression-molded in order to avoid the use of solvent, which can enhance crystallization.[75] The pellets were first dried in a vacuum oven at 150°C ($\approx T_g$) for 24 h before processing. A Carver laboratory hot press was set at 270 °C (above the melting point of polycarbonate, $T_m$, measured at 267 °C). Nitrogen gas was provided in the box containing the hot press in order to avoid any degradation of the polymer by oxidation at the processing temperature. Dried polycarbonate pellets were placed on Kapton polyimide sheets, sandwiched between flat metal plates, and the resulting mold was placed in the hot press. The same processing conditions (temperature, time, pressure) were maintained throughout to ensure reproducibility in the sample preparation. Once melted, the mold was removed from the hot press and quenched by blowing air. The polymeric films made by compression-molding were kept in a desiccator at all times to avoid any water moisture uptake. The thickness of the polycarbonate films averaged around 130 $\mu$m.

*Cooling Rate Protocol.* Prior to experiments, the polymeric films were put between thin Kapton sheets sandwiched between copper metal plates and suspended in the center of a Fisons gas chromatograph (GC) oven. The GC oven was equipped with an internal fan, and therefore heat transfer was assumed to be excellent on both sides of the metal plates sandwiching the polymer. The oven temperature was controlled within 1 °C. As shown in Figure 2, the samples were heated in the GC oven from 30 to 165 °C at a heating rate of 40 °C/min, kept at 165 °C for 15 min to remove thermal history and eliminate possible orientation, and cooled within the GC oven at a programmed rate to 30 °C. It was determined that 15 min was sufficient to remove thermal history. The room temperature was assumed to be low enough ($T_g$ − 120 °C) to freeze in the material during the time frame of the experiments.[39]

The programmed cooling rates were 0.5, 10, and 40 °C/min. However, the rate of cooling was strictly linear with time for a cooling rate of 10 °C/min and below only. At a cooling rate of 40 °C/min, the temperature profile decayed exponentially with time. Nevertheless, the experimental data were reproducible for a given cooling rate. The system was also cooled by opening the door of the GC oven and by blowing air immediately inside the oven with an external fan. The power of the fan, which was controlled by a variable autotransformer, was set at the maximum power. The polymer was believed to

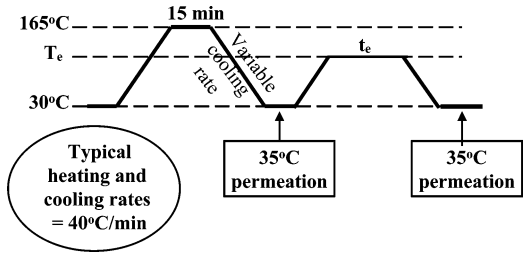


**Figure 2.** Schematic of the temperature program for the cooling rate studies. The polycarbonate films were heated from room temperature (30 °C) to 165 °C at a heating rate of 40 °C/min, kept at 165 °C for 15 min to remove thermal history, and cooled with the internal fan oven at several controlled rates to room temperature. The cooling rates were taken as 0.5 °C/min, 10 °C/min, 40 °C/min, or in excess of 40 °C/min (external fan).

cool faster than when cooled by the internal fan located inside the GC oven, and therefore the cooling rate was assumed in excess of 40 °C/min. Precautions were taken to maintain reproducibility between samples. The polymer films were used immediately once taken out of the GC oven.

*Physical Aging Protocol.* As outlined in Figure 2, the cooled samples were heated in the internal fan oven from room temperature to the sub-$T_g$ annealing temperature $T_e$ = 120 °C at a heating rate of 40 °C/min, kept at $T_e$ for a defined annealing time $t_e$, and again cooled within the oven at a cooling rate of 40 °C/min to room temperature. Permeation was performed immediately at 35 °C on the aged films. No change in thickness could be detected after sub-$T_g$ annealing.

**Instrumental Methods.** *Density.* The densities were obtained at 18 °C using a linear density gradient column made of an aqueous solution of sodium bromide. The sodium bromide NaBr salt was purchased from Aldrich Chemical Co. Its density was given as 3.203 g/cm$^3$. The salt was kept in a desiccator from the time of purchase until use to avoid water moisture uptake. The water was distilled water for high-performance liquid chromatography (HPLC) grade with a density of exactly 1 g/cm$^3$. Details about the preparation of the density gradient column can be found elsewhere.[76]

The theoretical resolution of the column was calculated to be about $5 \times 10^{-5}$ g/cm$^3$. At least three samples for each cooling rate treatment were dropped in the column to verify reproducibility.

*Dynamic Mechanical Thermal Analysis (DMTA).* The dynamic mechanical experiments were carried out in the tensile mode under atmospheric air. GPC analysis suggested that the samples were not degraded by oxidation during the time frame of the experiments. The machine was a DMTA IV from Rheometric Scientific.

Polycarbonate samples were cut with a mold into a rectangular shape. The dimensions of the samples were typically 25 × 4 mm, minimizing edge effects. The gap between the grips of the tensile apparatus was set as 12 mm. The thickness of the samples was assumed to be thin enough to avoid gradients of temperature in the samples while measuring dynamic properties. The position of the thermocouple remained unchanged between runs to ensure comparison between samples. The temperature inside the DMTA apparatus was controlled within 0.1 °C.

Dynamic temperature ramp experiments were carried out with the following conditions. A torque of 0.10 N m was used on each clamp. The frequency was chosen as 1 Hz, the heating rate as 2 °C/min, the initial temperature as 25 °C, the strain as typically 0.025%, and the static force as 33*g*. The static force was optimized by running dynamic frequency sweep test (strain control) at room temperature. In the aging experiments an extremely low strain level of 0.004% was selected in order to avoid any structural rearrangements that may occur at a higher strain level and hence destroy aging. The data were reproducible within 0.3%. For each cooling rate treatment, at least two samples were run in the DMTA to verify reproducibility.

Dynamic time sweep tests were performed on samples cooled at different rates. A torque of 15 CN m was used on each clamp. The static force was determined at the chosen annealing temperature $T_e$ by dynamic frequency sweep test (strain control). The strain chosen was typically 0.025%. The sample was left for 5 min at $T_e$ before starting the test itself in order to reach the desired annealing temperature $T_e$. The resulting force at 3 Hz was recorded for further testing. Once the previous test was finished, the gap between the grips was put back to 12 mm without opening the compartment of the DMTA in order to maintain the temperature at $T_e$. Dynamic time sweep experiments were immediately carried out with the following conditions. The frequency was set at 3 Hz, the strain at 0.025%, the static force as determined above, and the temperature at the annealing temperature $T_e$. Data were collected every 10 s for 20 h. GPC analysis verified that the samples did not degrade after this time at $T_e$. For each cooling rate treatment, at least two samples were run in the DMTA to verify reproducibility.

*Gas Permeation.* Permeation experiments were carried out using the permeation integral method.[88,89] The closed volume permeation apparatus utilized in our laboratory has been described in an earlier publication.[79]

Permeation experiments were carried out at 35 °C using He, $O_2$, and $N_2$, all supplied at 99.99% purity. These gases were expected to interact only weakly with the polymer hence, minimizing polymer swelling. Three measurements were taken per each gas and averaged for analysis. Each gas was passed through a molecular sieve prior to reaching the permeation apparatus itself in order to remove any water or oil. The applied pressures were fixed at 2.5 atm for He and 3.9 atm for $O_2$ and $N_2$. These pressures were low enough to assume the validity of Henry's law.[1]

Permeation experiments were carried out before and after physical aging on the same membrane. Once permeation data were obtained on the fresh sample, the membrane was degassed for a few hours before being placed in the oven for sub-$T_g$ annealing. This ensured that the gas trapped inside the polymeric matrix did not interfere with the typical aging process.

Permeation experiments were performed consecutively on the same membrane at 35, 55, 65, and 80 °C (cooling rate studies), and at 35, 40, 45, and 55 °C (physical aging studies), to determine the activation energies for gas transport. Each membrane was degassed for about 4 h before collecting data at a new temperature. Aging and deaging were found to be negligible at those temperatures within the time frame of the experiments. Indeed, no significant change in density or in the DMTA traces could be observed. In addition, the resulting data points did fit well on the Arrhenius plots.

## Results and Discussion

**Effect of Cooling Rate on Gas Transport and Other Physical Properties.** Similar to the conditioning by $CO_2$, the cooling rate from the rubbery state to the glassy state is an important processing parameter, since it affects the amount of free volume and its size distribution present in the polymeric material. The faster the cooling rate from a given temperature above $T_g$, the greater is the amount of free volume trapped inside the polymeric matrix.[80] This is demonstrated in Figure 3, which shows how the polycarbonate density drops with the cooling rate. The variation in the density values with cooling rate is in agreement with values reported in the literature.[62,80]

The gas transport coefficients of helium (He), oxygen ($O_2$), and nitrogen ($N_2$) were determined as a function of the cooling rate. The kinetic diameters of He, $O_2$, and $N_2$ are reported as 2.6, 3.46, and 3.64 Å, respectively.[81] The diffusion coefficients and solubility values were determined using the time-lag method and are summarized along with the permeabilities in Table 1. These

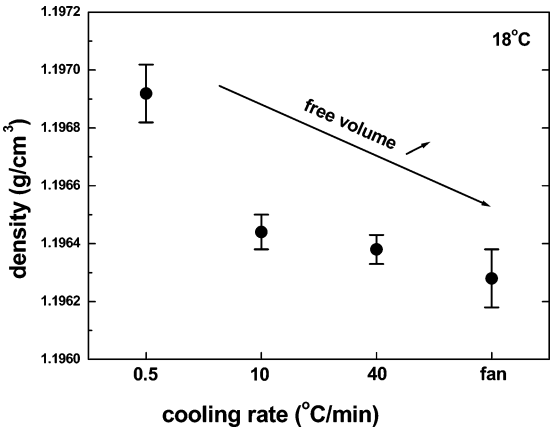


**Figure 3.** Density as a function of the cooling rate. The densities were measured at 18 °C using a linear density gradient column.

values are in agreement with the gas transport coefficients in polycarbonate reported in the literature.[17,82−85] Although, the permeability remained effectively unchanged with increasing cooling rate, the diffusion and solubility coefficients varied considerably. This was especially prominent for the transport coefficients for $N_2$, which has the larger kinetic diameter. Interestingly, the $N_2$ solubility coefficient increased and the $N_2$ diffusion coefficient $D$ decreased with increasing cooling rate, as shown in Figure 4 for $N_2$. The error bars for each gas reflect the accuracy between three successive gas transport measurements. As expected, the solubility increased with free volume. However, the behavior of the diffusion coefficient seems to be in contradiction with the free volume arguments proposed by Cohen and Turnbull.[5] On the other hand, our results are consistent with the work of Pekarski and co-workers,[48] who have observed decreasing diffusion coefficients with increasing free volume upon conditioning polycarbonate with $CO_2$.

Small molecule diffusion across a polymer membrane occurs by a series of activated jumps made by the gas molecule. Since polymer chains move constantly due to thermal motions, temporary channels open for a short period of time (of about a few hundred picoseconds[86]) and allow the gas molecules to move to adjacent cavities. The opening of the temporary channels involves only a few local polymeric segments or a low level of cooperativity. If these motions are constrained as a result of rapid quenching to a nonequilibrium state, we would expect the rate of diffusion to indeed decrease.

Kovacs and co-workers[87] and Tool[88] have shown that a distribution of relaxation times must exist in polymers, each relaxation time corresponding to a particular mode of molecular motion. If a polymeric sample is cooled slowly, the fast processes with short relaxation times are first to fully relax, resulting in a truncated relaxation time distribution spectrum.[87,89] Likewise, quenching should lead to broad distributions in the relaxation spectrum.

The activation energies of permeation, $E_P$, and diffusion, $E_D$, of He, $O_2$, and $N_2$ as a function of the cooling rate are shown in Figure 5 and Figure 6. As expected, $N_2$ with the largest kinetic diameter has the highest activation energy and shows greater sensitivity to the processing kinetics, its activation energy of diffusion increasing with the cooling rate. In a recent molecular modeling study of glassy polymers, Ford[49] has shown that the effects of polymer flexibility are reflected most significantly in the energy barriers to diffusional jumps. Thus, one would expect that the activation energy of diffusion should reflect the change in conformational energy necessary to open a diffusion path. For example, typical conformational energy changes associated with the motion of the carbonate group in the $\beta$ process are on the order of 10 kcal/mol.[90] This is on par with the observed change in the activation energy for diffusion for $N_2$, which is approximately 7 kcal/mol. Interestingly, perhaps because $O_2$ and He are smaller and more spherical, the diffusion and permeation of these molecules is not as much affected by the changes in the local fluctuations of molecular segments.

**Effect of Physical Aging on Gas Transport and Other Physical Properties.** The aging process was carried out as a function of time at a constant temperature of 120 °C on all four samples initially subjected to the varied cooling rates.

Changes in density with aging time at 120 °C were clearly observed, as shown in Figure 7 for the sample cooled at 40 °C/min. The density was found to increase linearly with the logarithm of the aging time $t_e$, reflecting a decreasing free volume as has been documented in the literature.[24−34] Quite interestingly, the changes seen in the density values with sub-$T_g$ annealing are of the same order of magnitude as those observed in the cooling rate studies reported above. Therefore, if the permeability coefficient is indeed related to the free volume content as postulated in the literature,[7,8] the permeability coefficient should be affected the same way by the cooling process as by the aging process. The densification rate was evaluated to be around 0.000 34 g/cm$^3$ for 1 decade for the samples cooled at 40 °C/min. For comparison, the densification rates evaluated from specific volume data[62] were estimated to be about 0, 0.000 177, and 0.000 35 g/cm$^3$ per decade for polycarbonate samples cooled at 1, 10, and 80 °C/min, respectively. Our results are therefore in agreement with the literature.[62] Accordingly, the greater the initial free volume content, the greater is the loss of this free volume with physical aging.

Changes in molecular dynamics and physical morphology can be probed by employing dynamic mechanical analysis (DMTA).[91,92] Although the effects of aging have been reported to be difficult to observe with DMTA because of the elevated frequencies involved in the experiments, we were able to characterize the aging of polycarbonate employing an extremely low strain level of 0.004%. This condition was selected in order to avoid any structural rearrangements that may occur at a higher strain level, destroying any aging effects. As the DMTA response of the loss modulus $E''$ was more sensitive than that of the storage modulus $E'$, only $E''$ is shown. As seen in Figure 8, the width of the $E''$ peak decreased with aging and the $E''$ peak shifted toward higher temperatures. These observations can be attributed to the decrease in the amount of free volume with aging, as suggested by the Fox and Flory theory[93,94] as well as to shifts in the relaxation times associated with higher activation energies.

Unfortunately, whenever a constant heating scan mode is used, interpretation of the aging results becomes complicated because of the interaction of this heating scan with the aging process. The structure of the original sample can change, especially at tempera-

**Table 1**

| | | cooling rate | | | |
|---|---|---|---|---|---|
| | | 0.5 °C/min | 10 °C/min | 40 °C/min | external fan |
| $P$ (barrer) | $P_{He}$ | 14.1 ± 0.35 | 14.6 ± 0.73 | 14.31 ± 0.36 | 14.08 ± 0.35 |
| | $P_{O_2}$ | 1.89 ± 0.05 | 1.99 ± 0.10 | 1.92 ± 0.05 | 1.91 ± 0.05 |
| | $P_{N_2}$ | 0.39 ± 0.01 | 0.41 ± 0.02 | 0.38 ± 0.01 | 0.39 ± 0.01 |
| | $P_{He}/P_{O_2}$ | 7.5 | 7.3 | 7.5 | 7.4 |
| | $P_{He}/P_{N_2}$ | 36.2 | 35.6 | 37.7 | 36.1 |
| | $P_{O2}/P_{N_2}$ | 4.8 | 4.9 | 5.1 | 4.9 |
| $D$ (cm²/s) | $D_{O_2}$ | 7.70E−08 ± 3.85E−09[a] | 8.16E−08 ± 8.30E−09 | 8.09E−08 ± 4.05E−09 | 6.97E−08 ± 3.49E−09 |
| | $D_{N_2}$ | 3.52E−08 ± 1.76E−09 | 3.40E−08 ± 3.40E−09 | 3.19E−08 ± 1.60E−09 | 2.62E−08 ± 1.31E−09 |
| | $D_{O_2}/D_{N_2}$ | 2.2 | 2.4 | 2.5 | 2.7 |
| $S$ (cm³ (STP)/ cm³ cmHg) | $S_{O_2}$ | 2.9E−03 ± 7.3E−05 | 2.9E−03 ± 1.4E−04 | 2.8E−03 ± 7.0E−05 | 3.3E−03 ± 8.1E−05 |
| | $S_{N_2}$ | 1.3E−03 ± 3.3E−05 | 1.5E−03 ± 7.0E−05 | 1.4E−03 ± 3.6E−05 | 1.8E−03 ± 4.5E−05 |
| | $S_{O2}/S_{N_2}$ | 2.2 | 2.0 | 2.0 | 1.8 |

[a] Read as $7.70 \times 10^{-8} \pm 3.85 \times 10^{-9}$.

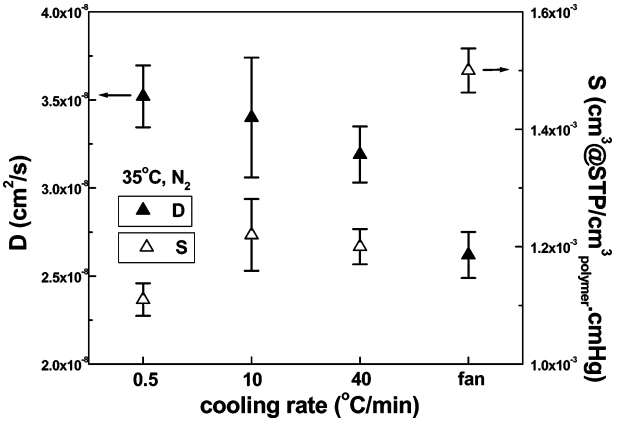


**Figure 4.** Diffusion coefficient $D$ and solubility coefficient $S$ for $N_2$ as a function of cooling rate. The permeation experiments were performed at 35 °C. The applied pressure was fixed at about 3.9 atm for $N_2$.

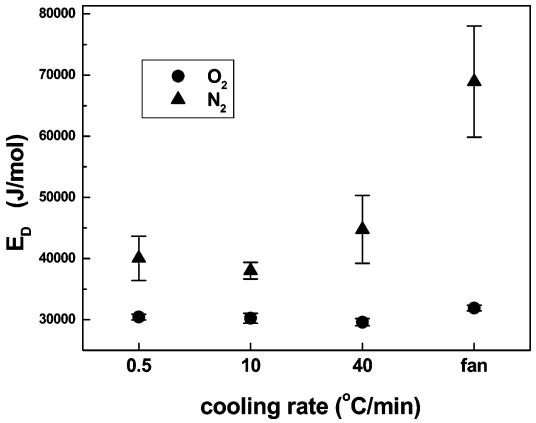


**Figure 6.** $E_D$ as a function of the cooling rate for $O_2$ and $N_2$. The applied pressure was fixed at about 3.9 atm for both $O_2$ and $N_2$. Permeation experiments were consecutively performed on the same membranes at 35, 55, 65, and 80 °C.

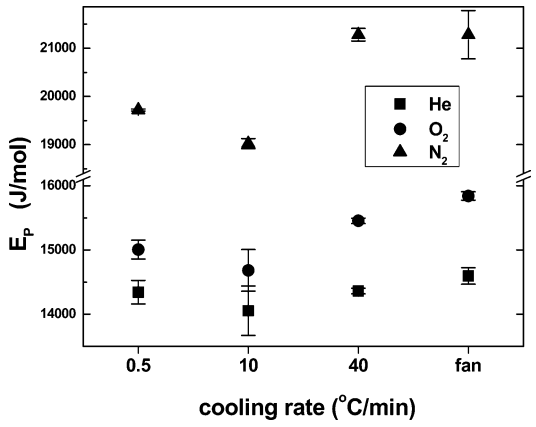


**Figure 5.** $E_P$ as a function of the cooling rate for He, $O_2$, and $N_2$. The applied pressures were fixed at about 2.5 atm for He and 3.9 atm for both $O_2$ and $N_2$. Permeation experiments were consecutively performed on the same membranes at 35, 55, 65, and 80 °C.

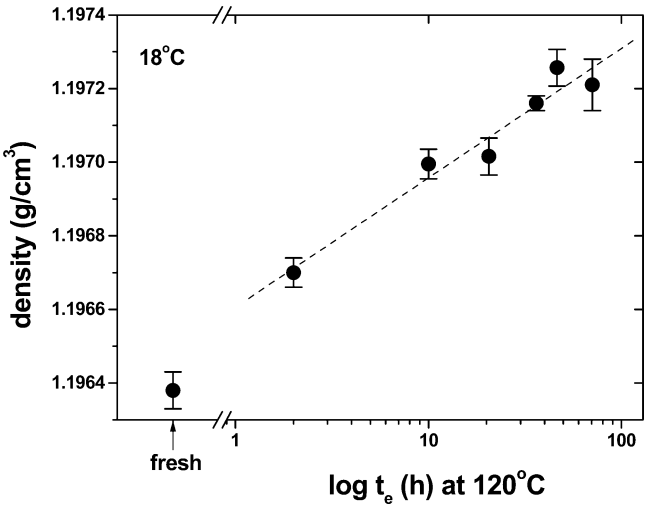


**Figure 7.** Density as a function of the aging time for a sample cooled at 40 °C/min and aged at 120 °C. The densities were measured at 18 °C using a linear density gradient column.

tures close to the $T_g$, thereby erasing any aging effects. Hence, we have also carried out isothermal DMTA experiments at 120 °C as a function of the annealing time on the samples cooled at different rates. The resulting DMTA traces showing tan $\delta$ for samples prepared using different cooling rates are provided in Figure 9. As expected, the samples cooled faster and thus containing the greatest amount of free volume aged faster. Moreover, the behavior became linear with the logarithm of the annealing time $t_e$ for the slow-cooled sample only. The initial increase in tan $\delta$ observed in Figure 9 at annealing times under 0.3 h is attributed to slight temperature fluctuations as the sample reached the equilibrium temperature. These results suggest that annealing the quenched sample should lead to the largest changes in the diffusion and solubility coefficients, if these properties are truly dependent on the free volume content.

Permeation studies were carried out before and after aging polycarbonate samples, initially cooled at 40 °C/min. No change in thickness could be detected with

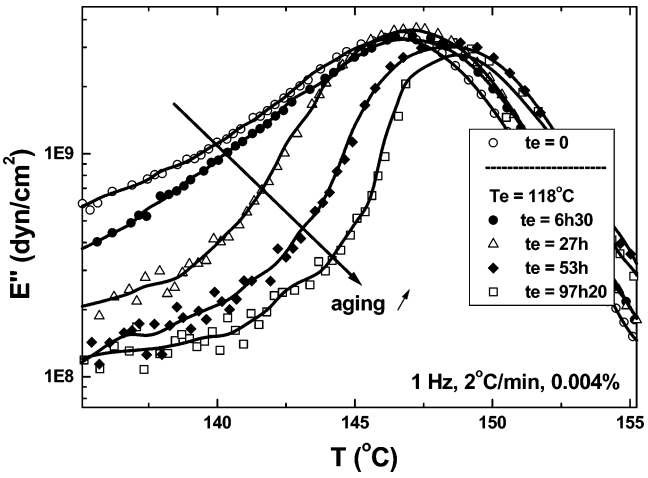


**Figure 8.** Effect of aging at 118 °C on the loss modulus of polycarbonate. The DMTA conditions were the following: frequency = 1 Hz, strain = 0.004%, initial temperature = 25 °C, heating rate = 2 °C/min, torque = 10 CN m. Samples were tested in the DMTA in a random order.

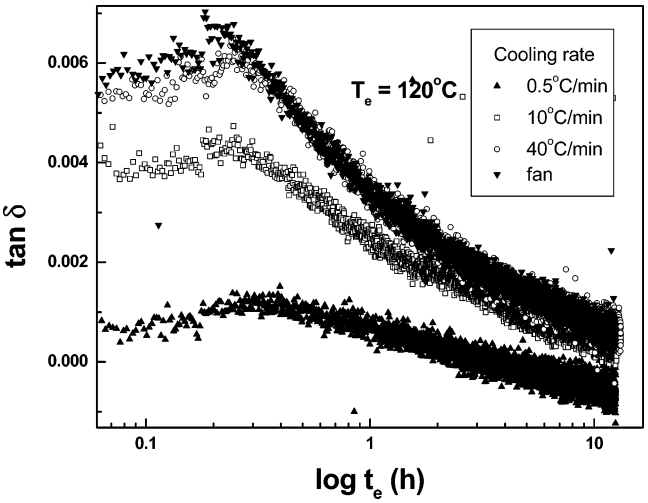


**Figure 9.** Tan $\delta$ as a function of the annealing time $t_e$ for the samples cooled at different cooling rates. The annealing temperature $T_e$ was chosen as 120 °C. The DMTA conditions were the following: frequency = 3 Hz, strain = 0.025%, data points collected every 10 s.

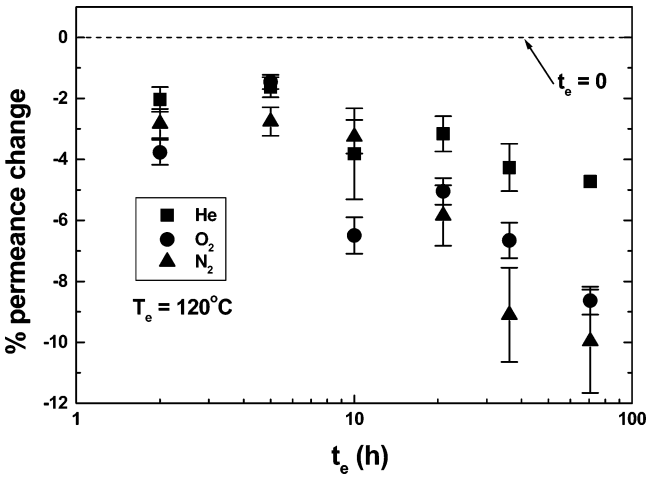


**Figure 10.** Percentage of the permeance change as a function of annealing time at 120 °C for the gases studied in this research. The permeation slopes were obtained at 35 °C and averaged. As apparent from the figure, the permeation slope was reduced with annealing time.

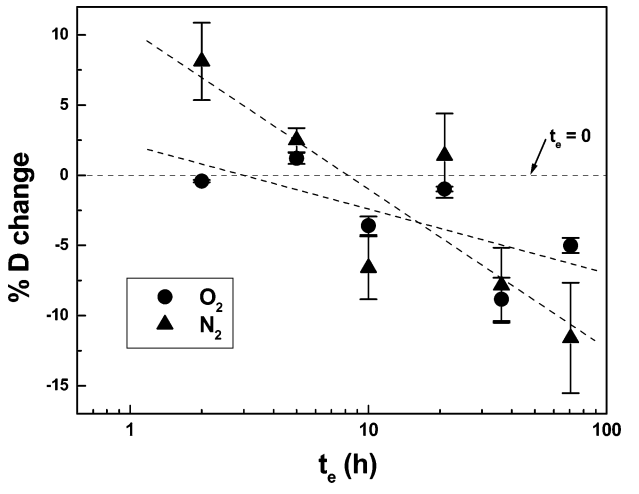


**Figure 11.** Percentage of diffusion coefficient $D$ change as a function of annealing time at 120 °C for the gases studied in this research. The permeation slopes were obtained at 35 °C and averaged for each gas.

sub-$T_g$ annealing. As expected, the permeation rate decreased after physical aging, particularly for the larger gases. To quantify these changes, we have calculated the percent relative change in the permeation upon aging. Permeance has units of $cm^3$ (STP)/($cm^2$ s cmHg). These percentages are plotted as a function of the annealing time as shown in Figure 10. The slope decreased for all three gases. Again, the greater the kinetic diameter of the gas, the greater was the decrease in the permeation profile. The separate effects of aging on the diffusion and the solubility coefficients are shown as percent change in Figure 11 and Figure 12, respectively. With the exception of one data point, the diffusion coefficient appears to decrease with aging for both $O_2$ and $N_2$ at longer times, which would seem to be consistent with the free volume theory and the density results. However, the decrease in the diffusion coefficients can also be correlated with the narrowing of the molecular relaxation times, which would also be consistent with the DMTA data. From a molecular point of view, this would mean that the segmental motion of the polymer chains would be more restricted with aging time, discriminating against molecules with increasing kinetic diameter. For example, it has been established that the carbonate groups in amorphous polycarbonate exist primarily in either the trans−trans or the trans−cis conformation.[65,66] During sub-$T_g$ annealing the population of trans−trans conformers increases whereas that of trans−cis conformers decreases.[65,66] These are not direct conformational rearrangements but rather a narrowing of the distribution of conformations around the trans−cis and the trans−trans conformations, achieved by extremely local rearrangements around the local energy minima. The trans−trans conformation is also known to be more energetically stable, while the number of trans−cis conformations increases with temperature.[65,66]

The error bars on the solubility coefficient limit accurate analysis of the data. However, it is safe to conclude that in general the solubility decreases with aging. This would be consistent with the overall decrease in free volume reflected in the density values. The solubility coefficient for $O_2$ stays relatively unchanged with annealing time. These results may also reflect changes in the shape of the free volume voids.

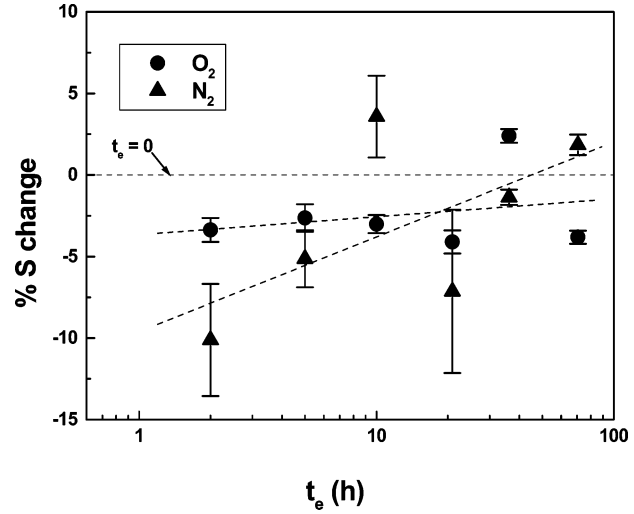


**Figure 12.** Percentage of solubility coefficient *S* change as a function of annealing time at 120 °C for the gases studied in this research. The permeation slopes were obtained at 35 °C and averaged for each gas.

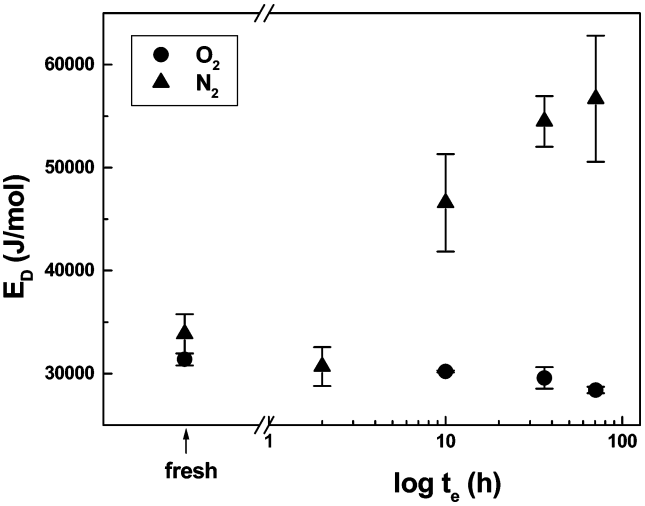


**Figure 13.** $E_D$ as a function of annealing time at 120 °C for the gases studied in this research. The permeation experiments were carried out at 35, 40, 45, and 55 °C. At $t_e = 2$ h, permeation experiments were carried out for $N_2$ only.

Gas transport activation energies were determined for the samples aged as a function of time at 120 °C and are shown in Figure 13 and Figure 14. The activation energy of permeation $E_P$ remained relatively constant with aging for all three gases. However, while $E_D$ and $\Delta H_s$ appear to remain constant with aging for $O_2$, $E_D$ increased and $\Delta H_s$ decreased significantly for $N_2$. This result means that more energy is necessary to dilate the chains and enable the diffusion process to take place. The decrease in $\Delta H_s$ with aging may be caused by the distribution in the free volume cavity sizes and shapes with aging. For example, it should require less energy for $N_2$ to sorb into larger free volume cavities.

Finally, we compare the effects of aging on polycarbonate samples cooled at different rates and hence starting at different thermodynamic states. All samples were aged at $T_e = 120$ °C for $t_e = 10$ h. Permeation results are shown as a function of the cooling rate in Figure 15 for $N_2$. The decrease in permeation after 10 h of annealing at 120°C depends largely on the starting thermodynamic state. In contrast with previous properties such as density and tan $\delta$ showing that the quenched sample aged the fastest, Figure 15 shows that the permeation of $N_2$ through the quenched sample was the least affected by aging. Again, these permeation data demonstrate behavior quite contrary to the free volume model. The separate responses observed for the diffusion *D* and the solubility *S* coefficients of $O_2$ and $N_2$ are shown in Figure 16 and Figure 17. The diffusion coefficients of $O_2$ and $N_2$ increased after annealing the quenched sample for 10 h at 120 °C; however, the other three samples had a decrease in *D* after the same time at 120 °C. At slower cooling rates, the decrease in *D* was more pronounced and more sensitive to the size of the penetrant. The solubility coefficient *S* of the quenched sample exhibited the highest decrease as would be consistent with the density and tan $\delta$ results. On the other hand, the solubility increased for $N_2$ in samples cooled from 0.5 to 40 °C/min. The diffusion and solubility coefficients of $O_2$ and $N_2$ can provide information on the structural rearrangements and scales taking place in polycarbonate with physical aging. While the solubility coefficients seem to reflect changes in free volume, we cannot help but believe that the diffusion coefficients are more sensitive to the relaxation state of the polymer chains. The greatest change in the diffusion coefficients

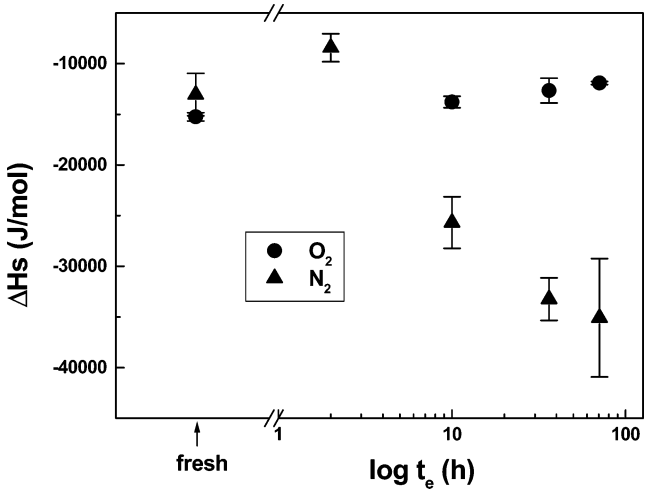


**Figure 14.** $\Delta H_s$ as a function of annealing time at 120 °C for the gases studied in this research. The permeation experiments were carried out at 35, 40, 45, and 55 °C. At $t_e = 2$ h, permeation experiments were carried out for $N_2$ only.

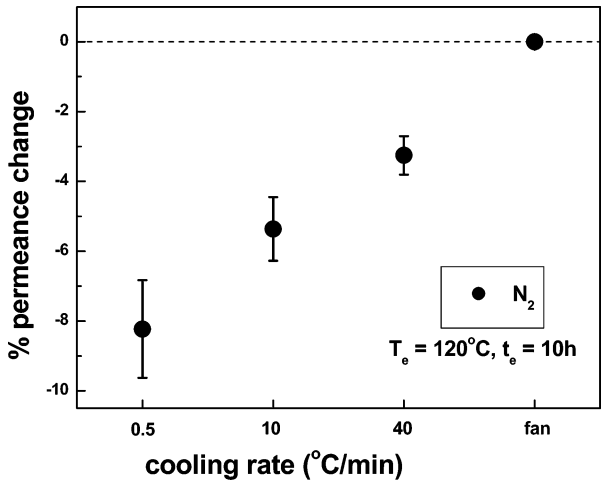


**Figure 15.** Percent in permeance change as a function of the cooling rate for $N_2$. The samples had been annealed at 120 °C for 10 h. The permeation experiments were carried out at 35 °C. The applied pressure was taken as 3.9 atm for $N_2$.

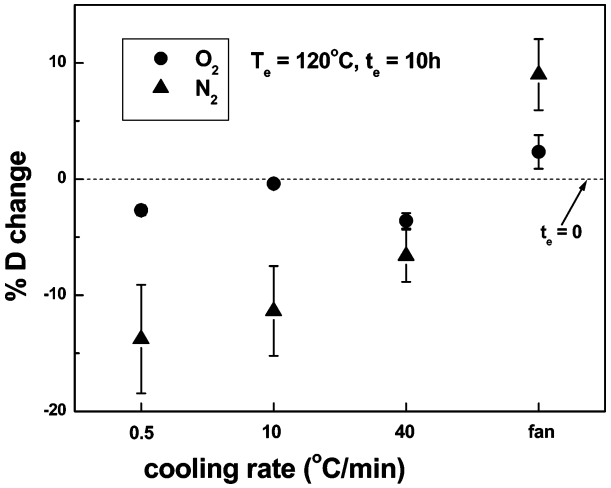


**Figure 16.** Percent in diffusion coefficient change as a function of the cooling rate for the various gases of interest. The samples had been annealed at 120 °C for 10 h. The permeation experiments were carried out at 35 °C.

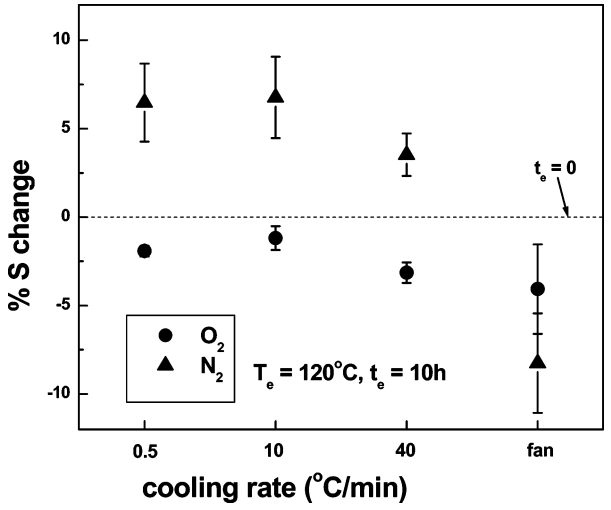


**Figure 17.** Percent in solubility coefficient change as a function of the cooling rate for the various gases of interest. The samples had been annealed at 120 °C for 10 h. The permeation experiments were carried out at 35 °C.

upon aging occurs in those polymers cooled very slowly. Because the amplitudes of molecular motions or degrees of freedom are initially high, they are suppressed to a greater extent with aging time. This is because physical aging is a self-retarding process. Furthermore, the polymer chains already in the lowest energy conformation, the trans−trans conformation, may with time align on a local scale, progressively loosing their degrees of freedom resembling the crystallization process. In contrast, the quenched polycarbonate sample responds very slowly to the annealing process because its polymer segments are in a strained conformational state. These segments must first disengage before they can relax to more stable conformations. Hence, the diffusion coefficients increase at short annealing times.

On the other hand, the solubility coefficients should reflect the changes in the free volume and free volume distribution with annealing time. The data suggest that with aging the size distribution of the cavities may become narrower, favoring the formation of cavities more accommodating to the $N_2$ gas molecules. Such cavities could be formed by cavity coalescence or by the reduction in the size of larger cavities. In addition, a reduction in the overall volume of the cavities has to occur in order to account for the increase in density. Published data concerning physical aging have shown a decrease in the sorption properties of the polymer with aging,[40,70] in contrast to our results with the exception of the quenched samples. The published data are, however, complicated by several factors, such as conditioning, samples used as-received or cast from solution, plasticization induced by carbon dioxide, and the nature of the sorption experiment. The average hole size has been determined by two-dimensional angular correlation of annihilation radiation (2D-ACAR) to be about 2.9 Å for polycarbonate,[95] which is in the range of the kinetic diameters of $O_2$ (3.46 Å) and $N_2$ (3.64 Å). Since both $P$ and $D$ decrease with aging and $P = DS$, then it appears that the changes in permeability are more reflective of the changes in diffusivity.

The fact that the samples cooled slowly and thus containing the lowest amount of free volume show a greater decrease in the permeability coefficient with sub-$T_g$ annealing seems somehow similar to the "mobility paradox" observed for annealed oriented polycarbonate samples.[50,96,97]

**Toward a Theoretical Model.** Our experimental data suggest that the changes in free volume have less of an effect on diffusion coefficients than the changes arising from the distribution of energy barriers associated with local polymer motion. Here, we present a simple model, which provides some theoretical support for this hypothesis. Since it is based on an extremely simplified description of the polymer membrane, our conclusions—while intriguing—should be considered preliminary until further studies[98] are completed. At the current stage of the modeling process, they should serve as a proof of principle only, namely, that diffusivities can be controlled by energy barriers alone and free volume need not come into play. Since the observed density changes in the polycarbonate were so small, this reasoning can be equally applied to the permeability results as well.

Since we do not observe any aging or deaging effects during the time frame of the permeation experiments, we model the membrane as a static network of monomers. The real network is of course three-dimensional. Two directions are transverse, and one is parallel to the applied density gradient of gas particles. Our first crude simplification is to adopt a one-dimensional description: we imagine that the polymer network is just a system of one-dimensional channels, aligned with the longitudinal direction. The gas particles are assumed to diffuse through these channels and are not allowed to jump from one channel to a neighboring one. In other words, we neglect transverse diffusion of the gas.

Modeling the channels as noninteracting, it is now sufficient to consider a single one, since the total particle current through the membrane is obviously proportional to the current through a single channel. We model the channel as a one-dimensional lattice of sites (identical "voids", $i = 1, 2, ..., N$), each of which can be occupied by a limited number of gas particles. Neither the number of voids nor their maximum occupation will change in the following, so that the total available free volume remains constant. The lattice constant is denoted by $a$, so that the thickness, $L$, of the membrane determines $N$ via $N = L/a$. The local number density of

particles at site $i$ and time $t$ is denoted by $\rho_i(t)$, with $0 \le \rho_i(t) \le 1$. Here, $\rho_i(t) = 0$ (1) denotes a completely empty (full) void. Neighboring sites are separated by (random) activation energy barriers, $E_i$, whose distribution will be specified later. For now, we simply consider the rate $R_i \propto \exp(-E_i/kT)$ with which a particle attempts to jump between sites $i$ and $i + 1$ as given. (The conventional activation energy theory involves both site energies and barrier heights (saddle point energies), so that the jump rates for $i \rightarrow j$ and $j \rightarrow i$ will differ in general. To model our process in quantitative detail, these considerations will be of course crucial. However, it is sufficient to assume equal forward/backward rates for the purposes of this section, i.e., to demonstrate the important effects of a *distribution* of barrier energies on permeabilities.) Whether the jump actually takes place is proportional to the particle density at the originating site and the available "space" at the receiving site. Thus, the equation of motion for $\rho_i(t)$ takes the form

$$\frac{\mathrm{d}}{\mathrm{d}t}\rho_i(t) = R_{i-1}[\rho_{i-1}(1-\rho_i) - (1-\rho_{i-1})\rho_i] - R_i[\rho_i(1-\rho_{i+1}) - (1-\rho_i)\rho_{i+1}]$$
$$= R_{i-1}(\rho_{i-1} - \rho_i) - R_i(\rho_i - \rho_{i+1}) \quad (1)$$

It is helpful to note that $R_i(\rho_i - \rho_{i+1})$ is just the particle current, $J_i$, across the barrier between sites $i$ and $i + 1$, so that eq 1 takes the form of a continuity equation. Obviously, the currents are proportional to the local rate and the density difference of the participating sites. The density of gas particles on the input (pressurized) and output sides of the membrane are modeled by two constants, $\rho_0$ and $\rho_{N+1}$, which serve as boundary conditions for eq 1. Gas particles enter and leave the membrane with rates $R_0$ and $R_N$, respectively.

Leaving the full time dependence to a later publication,[98] we focus on the stationary (long-time) limit which is characterized by a time-independent density profile, $\mathrm{d}\rho_i(t)/\mathrm{d}t = 0$. Equation 1 can then be solved by having $J_i$ being a constant for all $i$, corresponding to a *constant current* flowing through the channel. Denoting this constant by $J$, or $J(\{R_i\})$ to emphasize its dependence on the set of $R$'s, we write the standard, explicit expression

$$J \equiv J(\{R_i\}) = \left[\sum_{i=0}^{N}\frac{1}{R_i}\right]^{-1}(\rho_0 - \rho_{N+1}) \quad (2)$$

It is interesting to note the analogy with electric currents: If $(\rho_0 - \rho_{N+1})$ is the potential difference applied to the two ends of a wire, $1/R_i$ plays the role of a resistance, and we recognize eq 2 as the expression for the current through $N + 1$ resistors in series.

Continuing with our analysis, we can compute the stationary density profile across the channel:

$$\rho_i = \rho_0 - \sum_{k=0}^{i-1}\frac{J}{R_k} \quad (3)$$

This expression can be put into an especially intuitive form if we define

$$f_i \equiv \frac{\sum_{k=0}^{i-1}\frac{1}{R_k}}{\sum_{k=0}^{N}\frac{1}{R_k}} \quad (4)$$

with $0 \le f_i \le 1$. This allows us to write the local densities as appropriate fractions of the boundary densities:

$$\rho_i = (1 - f_i)\rho_0 + f_i\rho_{N+1} \quad (5)$$

Of course, this results in a simple linear equation if all $R_i$ are equal, namely, $\rho_i = \rho_0 - i(\rho_0 - \rho_{N+1})/N$ independent of $R_i$. Finally, the total number, $S$, of particles stored in the membrane can also be found easily:

$$S = \sum_{i=1}^{N}\rho_i = N\rho_0 - (\rho_0 - \rho_{N+1})\sum_{i=1}^{N}f_i = N\rho_0 - \frac{\rho_0 - \rho_{N+1}}{\sum_{k=0}^{N}\frac{1}{R_k}}\sum_{k=0}^{N}\frac{k}{R_{N-k}} \quad (6)$$

We now turn to the second part of our problem, namely, the effect of different distributions of barrier heights. Starting with the simplest possible model, we assume that (i) the local barrier heights $E_i$ are all equally distributed and uncorrelated and (ii) they obey a Gaussian distribution:

$$p(E) = \frac{1}{\sqrt{2\pi\sigma^2}}\exp[-(E - \bar{E})^2/2\sigma^2] \quad (7)$$

Note that this distribution is independent of the origin of the energy scale (a reference point). Nevertheless, to be clear for later considerations, let us assume that an arbitrary barrier has been chosen as a standard and associate its "height" with $E = 0$. With this choice, the energies $E_i$ should be regarded as differences with respect to this "standard height". To proceed, we conjecture that the average $\bar{E}$ and the width (standard deviation) $\sigma$ of this Gaussian both depend on cooling rate and annealing time. Before discussing the details of this dependence in the context of the experimental findings, it is instructive to compute the average current, for a given $\bar{E}$ and $\sigma$.

We begin by rewriting the current, for a specified set of $\{R_i\}$, in somewhat more manageable form, via the following integral:

$$J(\{R_i\}) = (\rho_0 - \rho_{N+1})\int_0^\infty \mathrm{d}\mu \prod_{i=0}^{N}\exp(-\mu/R_i) \quad (8)$$

It is easily checked that this form agrees with eq 2. Given a distribution for the $\{R_i\}$, $W(\{R_i\})$, we can write the *average current* as

$$\langle J\rangle = (\rho_0 - \rho_{N+1})\int_0^\infty \mathrm{d}\mu\ W(\{R_i\})\ J(\{R_i\})\prod_{i=0}^{N}\mathrm{d}R_i \quad (9)$$

Here, the notation $\langle\cdot\rangle$ refers to an average over different realizations of the $\{R_i\}$, weighted by the distribution $W(\{R_i\})$. Note that $\langle J\rangle$ is measured in the experiment

and is just proportional to the permeability:

$$P \propto \langle J \rangle$$

Invoking the first of our two assumptions, namely, that the $R$'s are uncorrelated and distributed identically, according to $p(R)$, we write $W(\{R_i\}) = p(R_0)...p(R_N)$, and eq 9 reduces to

$$\langle J \rangle = (\rho_0 - \rho_{N+1}) \int_0^\infty \mathrm{d}\mu \, [\int \mathrm{d}R p(R) \mathrm{e}^{-\mu/R}]^{N+1} \quad (10)$$

Next, we employ the second assumption, namely, eq 7, the Gaussian character of the *barrier* distribution. Though eq 10 contains $p(R)$ rather than $p(E)$, there is no need to find $p(R)$ explicitly, since $p(R)\,\mathrm{d}R$ is precisely $p(E)\,\mathrm{d}E$. The only extra step we need is to relate the $R$ in the exponential to $E$, i.e., $R = \bar{R} \exp(-\beta E)$, with $\beta = 1/kT$ and $\bar{R}$ being the rate associated with our standard barrier. Thus, $\langle J \rangle$ becomes

$$\langle J \rangle = (\rho_0 - \rho_{N+1}) \int_0^\infty \mathrm{d}\mu \left[ \frac{1}{\sqrt{2\pi\sigma^2}} \int_{-\infty}^{+\infty} \mathrm{d}E \, \exp\left( - \frac{(E - \bar{E})^2}{2\sigma^2} - \frac{\mu}{\bar{R}} \mathrm{e}^{\beta E} \right) \right]^{N+1} \quad (11)$$

Introducing more convenient variables

$$x \equiv \frac{E - \bar{E}}{\sigma}; \quad \lambda \equiv \mu \mathrm{e}^{\beta \bar{E}} / \bar{R} \geq 0 \quad (12)$$

and defining the integral

$$g(\lambda,\alpha) \equiv \int_{-\infty}^{+\infty} \mathrm{d}x \, \mathrm{e}^{-\lambda \exp(\beta\sigma x)} \frac{\mathrm{e}^{-x^2/2}}{\sqrt{2\pi}} \quad (13)$$

we finally arrive at the average current:

$$\langle J \rangle = \bar{J} \mathrm{e}^{-\beta\bar{E}} \int_0^\infty \mathrm{d}\lambda \, [g(\lambda,\beta\sigma)]^{N+1} (N+1) \quad (14)$$

Here

$$\bar{J} \equiv \frac{(\rho_0 - \rho_{N+1})\bar{R}}{N+1} \quad (15)$$

represents the current when all barriers are "standard", with the usual ingredients of pressure difference and the overall channel "length". Also displayed in eq 14 are the other two factors in our model. The first is associated with the average activation barrier, while the second, being a function of $\beta\sigma$ only, accounts for the spread in the barrier heights. Note that the integral in eq 14 is "normalized" to unity for $\sigma = 0$. Clearly, for fixed $\sigma$, the average current will increase when the average barrier height decreases, as expected. If, however, the *width* of the distribution increases, at fixed $\bar{E}$, both higher and lower barriers are probed: the analogy with resistors in series then suggests that the current will decrease due to the presence of higher barriers. Indeed, for large $N$, the integral in eq 14 can be computed approximately, so that

$$\langle J \rangle = \bar{J} \mathrm{e}^{-\beta\bar{E} - (1/2)(\beta\sigma)^2} + O(1/N^2) \quad (16)$$

which is a quantitative measure of our expectations. To summarize, we find that both larger widths and larger $\bar{E}$ reduces the current and, hence, the permeability. With these two parameters, we can model a range of permeabilities.

To put this into perspective, let us recall the pertinent experimental findings. According to Table 1, after the initial processing step, the membranes all have about the same permeability to a given gas, independent of cooling rate. Thus, in the theory we would have to adjust $\bar{E}$ and $\sigma$ such that $\beta_0\bar{E} + (\beta_0\sigma)^2/2 \approx$ constant with $\beta_0$ corresponding to 35 °C. Next, the data of Figure 5 have been obtained by fitting the permeabilities obtained as a function of temperature to a simple exponential, $\sim \exp(-\beta E_\mathrm{P})$, in the temperature interval 35−80 °C. To understand this behavior in the context of our model, we note that this range corresponds only to a small (∼10%) variation in the absolute temperature. Thus, in a plot of log $\langle J \rangle$ vs $\beta$, an approximate slope in this temperature range can be extracted. In other words, we would fit the derivative of the argument of the exponential in eq 16 to $E_\mathrm{P}$:

$$E_\mathrm{P} \cong \bar{E} + \beta_0\sigma^2 \quad (17)$$

Using this approach, the results in Figure 5 are consistent with the idea that the increase in activation energy for permeation in the quenched sample is due to increases in $\sigma$.

Finally, we observe (Figure 15) that the permeability decreases upon annealing and that the magnitude of the drop depends strongly on the cooling rate. If we adopt the above view that fast-cooled samples are characterized by a broader distribution of energy barriers than slow-cooled ones and that the distribution narrows upon annealing, then $\bar{E}$ must increase accordingly to compensate. Thus, *at least in principle*, our theoretical description is reconcilable with the data.

Of course, the behavior of a real, three-dimensional membrane is far more complicated. Upon cooling and annealing, energy barriers redistribute themselves, affecting transport not only along the parallel but also the transverse directions. Returning to our analogy with electric networks, this translates into dealing with a random network of resistors, including both series and parallel arrangements. While currents through resistors in series are dominated by the largest resistances (i.e., highest energy barriers), currents through resistors in parallel are dominated by the lowest resistances. Thus, changes in the barrier distribution for longitudinal and transverse diffusion are expected to compete in subtle ways. In particular, preliminary Monte Carlo simulations indicated that any random (uncorrelated) distribution of a fixed number of barriers over a square lattice results in the same value of the current. However, introducing correlations (due, e.g., to predominantly attractive monomer−monomer interactions) lowers the current. In the literature, Monte Carlo studies have been reported, of particles hopping through random environments, within the context of diffusion of hydrogen in metals.[99] However, the correlations between the impurities and defects in a metal are quite different from those of polymers in an aging matrix. Thus, we believe that the implications of our preliminary results, together with the simplicity of the model, warrant further investigation. There is also a recent study of particle diffusion through glassy polymers,[100] exploiting a theory of *uncorrelated* distributions of site energies[99] and applied to an experimental setup quite distinct from ours. In aging, serious correlations between the barrier

heights are expected to play an important role, so that theoretical and/or Monte Carlo studies of the effects of such correlations are desirable. Given the experimental data, one might be tempted to conjecture that relatively fast cooling results in different yet uncorrelated barrier distributions, while annealing allows correlations to build up. A full analysis of these features will be published elsewhere.[98]

## Conclusions

The results obtained in the cooling and aging studies lead us to believe that diffusion coefficients may correlate better with the activation energies associated with local polymer segmental motions, rather than with the overall free volume content. Diffusion coefficients in samples prepared by slow cooling from the rubbery state are higher because the polymer chains are less constrained. Fast cooling rates lead to highly restricted conformations, which limit segmental mobility and lower the rate of gas diffusion through the polycarbonate. In this case, the distribution of activation energies for diffusion is broad. Aging at sub-$T_g$ conditions further reduces segmental mobility and leads to a progressive loss in the degrees of freedom as the polymer chains align on a local level. The aging process occurs at a faster rate in the relaxed (slowly cooled systems) simply because of the higher initial segmental mobility. The permeability coefficient of slow-cooled samples decreased faster with physical aging than that of quenched samples, despite the lower densification rate. Aging of quenched polycarbonate can also reduce the segmental mobility, but because the segments are more constrained, this process occurs much more slowly than in relaxed systems. Comparisons between experimental results and theoretical consideration suggest that aging results in narrowing of the distribution in the activation energy for diffusion (permeation) and an increase in the mean activation energy. These effects are balanced in quenched samples leading to a net zero change in permeance.

**Acknowledgment.** We extend our sincere thanks to Dr. C. Cornelius for his invaluable advice, to Dr. Ji and Dr. Kim for carrying out GPC measurements, to Dr. Sohn for his advice about the compression-molding process, and to Dr. Alizadeh for her help with setting up the density gradient column. We also thank J. Das for preliminary simulation data. This work was supported by the National Science Foundation via Grants DMR-0088451 and CTS-9905549.

## References and Notes

(1) Ghosal, K.; Freeman, B. D. *Polym. Adv. Technol.* **1994**, *5*, 673−697.
(2) Vieth, W. R.; Howell, J. M.; Hsieh, J. H. *J. Membr. Sci.* **1976**, *1*, 177−220.
(3) Doolittle, A. K. *J. Appl. Phys.* **1951**, *22*, 1031.
(4) Doolittle, A. K. *J. Appl. Phys.* **1951**, *22*, 1471.
(5) Cohen, M. H.; Turnbull, D. *J. Chem. Phys.* **1959**, *31*, 1164.
(6) Fujita, H. *Fortschr. Hochpolym. Forsch.* **1961**, *3*, 1.
(7) Park, J. Y.; Paul, D. R. *J. Membr. Sci.* **1997**, *125*, 23−39.
(8) Yampolskii, Y.; Shishatskii, S.; Alentiev, A.; Loza, K. *J. Membr. Sci.* **1998**, *148*, 59−69.
(9) Lee, W. M. *Polym. Eng. Sci.* **1980**, *20*, 65−69.
(10) McHattie, J. S.; Koros, W. J.; Paul, D. R. *Polymer* **1991**, *32*, 5, 840−850.
(11) McHattie, J. S.; Koros, W. J.; Paul, D. R. *J. Polym. Sci., Part B: Polym. Phys.* **1991**, *29*, 731−746.
(12) Dorkenoo, K. D.; Pfromm, P. H.; Rezac, M. E. *J. Polym. Sci., Part B: Polym. Phys.* **1998**, *36*, 797−803.
(13) Mohr, J. M.; Paul, D. R.; Tullos, G. L.; Cassidy, P. E. *Polymer* **1991**, *32*, 2387−2394.
(14) Toi, K.; Suzuki, H.; Ikemoto, I.; Ito, T.; Kasai, T. *J. Polym. Sci., Part B: Polym. Phys.* **1995**, *33*, 777−784.
(15) Kim, H. J.; Hong, S. I. *Korean J. Chem. Eng.* **1999**, *16*, 343−350.
(16) Hensema, E. R.; Boom, A. P. *Macromol. Symp.* **1996**, *102*, 409−419.
(17) Thran, A.; Kroll, G.; Faupel, F. *J. Polym. Sci., Part B: Polym. Phys.* **1999**, *37*, 3344−3358.
(18) Jean, Y. C.; Yuan, J. P.; Liu, J.; Deng, Q.; Yang, H. *J. Polym. Sci., Part B: Polym. Phys.* **1995**, *33*, 2365−2371.
(19) Kobayashi, Y.; Haraya, K.; Hattori, S. *Polymer* **1994**, *35*, 925−928.
(20) Trohalaki, S.; DeBolt, L. C.; Mark, J. E.; Frisch, H. L. *Macromolecules* **1990**, *23*, 813−816.
(21) Maeda, Y.; Paul, D. R. *J. Polym. Sci., Part B: Polym. Phys.* **1987**, *25*, 1005.
(22) Paul, D. R., Yampol'skii, Y. P., Eds.; *Polymeric Gas Separation Membranes*; CRC Press: Boca Raton, FL, 1994.
(23) Kresse, I.; Usenko, A.; Springer, J.; Privalko, V. *J. Polym. Sci., Part B: Polym. Phys.* **1999**, *37*, 2183−2193.
(24) Struik, L. C. E. *Physical Aging in Amorphous Polymers and Other Materials;* Elsevier: New York, 1978.
(25) Tant, M. R.; Wilkes, G. L. *Polym. Eng. Sci.* **1981**, *21*, 874.
(26) Hutchinson, J. M. In *The Physics of Glassy Polymers*; Haward, R. N., Young, R. J., Eds.; Chapman & Hall: London, 1997.
(27) Hutchinson, J. M. *Prog. Polym. Sci.* **1995**, *20*, 703.
(28) Chartoff, R. P. In *Thermal Characterization of Polymeric Materials*, Turi, E. A., Ed.; Academic Press: New York, 1997; pp 548−573.
(29) Struik, L. C. E. In *Encyclopedia of Polymer Science and Engineering*; Wiley: New York, 1985; Vol. 1, pp 595−611.
(30) O'Reilly, J. M. *CRC Crit. Rev. Solid State Mater. Sci.* **1987**, *13*, 259−277.
(31) Mijovic, J.; Nicolais, L.; D'Amore, A.; Kenny, A. J. M. *Polym. Eng. Sci.* **1994**, *34*, 381.
(32) Matsuoka, S. *Polym. Eng. Sci.* **1981**, *21*, 907−921.
(33) Bauwens, J. C. In *Failure of Plastics*; Brostow, W., Corneliussen, R. D., Eds.; Hanser Publishers: Munich, 1986.
(34) Struik, L. C. E. In *Failure of Plastics*; Brostow, W. W., Corneliussen, R. D., Eds.; Hanser Publishers: Munich, 1986.
(35) Pethrick, R. A. *TRIP* **1993**, *1*, 226−227.
(36) Cowie, J. M. G.; Harris, S.; McEwen, I. J. *Macromolecules* **1998**, *31*, 2611−2615.
(37) Simon, S. L.; Plazek, D. J.; Harper, B. J.; Holden, T. *PSME Prepr.* **1997**, *76*, 334.
(38) Hutchinson, J. M.; Smith, S.; Horne, B.; Gourlay, G. M. *Macromolecules* **1999**, *32*, 5046−5061.
(39) Hachisuka, H.; Takizawa, H.; Tsujita, T.; Takizawa, A.; Kinoshita, T. *Polymer* **1991**, *32*, 2383.
(40) Chan, A. H.; Paul, D. R. *Polym. Eng. Sci.* **1980**, *20*, 87.
(41) Hachisuka, H.; Tsujita, Y.; Takizawa, A.; Kinoshita, T. *J. Polym. Sci., Part B: Polym. Phys.* **1991**, *29*, 11.
(42) Toi, K.; Ito, T.; Ikemoto, I. *J. Polym. Sci., Polym. Lett. Ed.* **1985**, *23*, 525−529.
(43) Nagai, K.; Nakagawa, T. *J. Membr. Sci.* **1995**, *105*, 261−272.
(44) Illers, Von K.-H. *Makromol. Chem.* **1969**, *127*, 1−33.
(45) Nakagawa, T.; Watanabe, T.; Mori, M.; Nagai, K. *Polym. Mater. Sci. Eng.* **1997**, *77*, 249.
(46) Hachisuka, H.; Kito, K.; Tsujita, Y.; Takizawa, A.; Kinoshita, T. *J. Appl. Polym. Sci.* **1988**, *35*, 1333.
(47) Smith, T. L.; Adam, R. E. *Polymer* **1981**, *22*, 299−304.
(48) Pekarski, P.; Hampe, J.; Böhm, I.; Brion, H. G.; Kirchheim, R. *Macromolecules* **2000**, *33*, 2192−2199.
(49) Rallabandi, P. S.; Thompson, A. P.; Ford, D. M. *Macromolecules* **2000**, *33*, 3142−3152.
(50) Shelby, M. D.; Hill, A. J.; Burgar, M. I.; Wilkes, G. L. *J. Polym. Sci., Part B: Polym. Phys.* **2001**, *39*, 32−46.
(51) Hill, A. J.; Katz, I. M.; Jones, P. L. *Polym. Eng. Sci.* **1990**, *30*, 762.
(52) Cheng, T. W.; Heskkula, H.; Paul, D. R. *J. Appl. Polym. Sci.* **1992**, *45*, 531−551.
(53) Schultheisz, C. R.; McKenna, G. B. *Polym. Mater. Sci. Eng.* **1997**, *76*, 221.
(54) Hill, A. J.; Heater, K. J.; Agrawai, M. *J. Polym. Sci., Part B: Polym. Phys.* **1990**, *28*, 387.
(55) Sandreczki, T. C.; Hong, X.; Jean, Y. C. *Macromolecules* **1996**, *29*, 4015−4018.
(56) Hill, A. J.; Agrawal, C. M. *J. Mater. Sci.* **1990**, *25*, 5036−5042.

(57) Kluin, J. E.; Moaddel, H.; Ruan, M. Y.; Yu, Z.; Jamieson, A. M.; Simha, R.; McGervey, J. D. In *Structure−Property Relations in Polymers: Spectroscopy and Performance*; American Chemical Society: Washington, DC, 1993; Vol. 236, pp 535−555.
(58) Sandreczki, T. C.; Homg, X.; Jean, Y. C. *Macromolecules* **1996**, *29*, 4015−4018.
(59) Kluin, J. E.; Yu, Z.; Vleeshouwers, S.; McGervey, J. D.; Jamieson, A. M.; Simha, R. *Macromolecules* **1992**, *25*, 5089.
(60) Stolarski, V.; Letton, A.; Nour, E.; Laane, J. *ANTEC'94* **1994**, 2077.
(61) Stolarski, V.; Letton, A.; Lee, S. N.; Laane, J. *Polym. Mater. Sci. Eng.* **1994**, *71*, 479−480.
(62) Wimberger-Friedl, R.; de Bruin, J. G. *Macromolecules* **1996**, *29*, 4992−4997.
(63) Curro, J. J.; Roe, R. J. *Polymer* **1984**, *25*, 1424.
(64) Royal, J. S.; Torkelson, J. M. *Macromolecules* **1992**, *25*, 4792.
(65) Lu, J.; Wang, Y.; Chen, D. *Polym. J.* **2000**, *32*, 7, 610−615.
(66) Heymans, N. *Polymer* **1997**, *38*, 14, 3435.
(67) Guerdoux, L.; Marchal, E. *Polymer* **1981**, *22*, 1199.
(68) Bauwens-Crowet, C.; Bauwens, J. C. *Polymer* **1986**, *27*, 709.
(69) Jordan, S. M.; Koros, W. J.; Beasley, J. K. *J. Membr. Sci.* **1989**, *43*, 103−120.
(70) Pope, D. S.; Fleming, G. K.; Koros, W. J. *Macromolecules* **1990**, *23*, 2988.
(71) Wonders, A. G.; Paul, D. R. *J. Membr. Sci.* **1979**, *5*, 63.
(72) Fleming, G. K.; Koros, W. J. *Macromolecules* **1990**, *23*, 1353.
(73) Tanaka, K.; Ito, M.; Kita, H.; Okamoto, K.; Ito, Y. *Bull. Chem. Soc. Jpn.* **1995**, *68*, 3011−3017.
(74) Jean, Y. C.; Hong, X.; Liu, J.; Huang, C. M.; Cao, H.; Chung, C. Y.; Dai, G. H.; Cheng, K. L.; Yang, H. *J. Radioanal. Nucl. Chem.* **1996**, *210*, 513−524.
(75) Alizadeh, A.; Sohn, S.; Quinn, J.; Marand, H.; Shank, L. C.; Iler, H. D. *Macromolecules* **2001**, *34*, 4066−4078.
(76) Laot, C. M. Gas transport properties in polycarbonate−Influence of the cooling rate, physical aging, and orientation. PhD Dissertation, Virginia Polytechnic Institute and State University, Oct 17, 2001.
(77) Felder, R. M. *J. Membr. Sci.* **1978**, *3*, 15.
(78) Pye, D. G.; Hoehn, H. H.; Panar, M. *J. Appl. Sci.* **1976**, *20*, 1921.
(79) Dhingra, S. S.; Marand, E. *J. Membr. Sci.* **1998**, *141*, 45−63.
(80) Wimberger-Friedl, R.; Prast, G.; Kurstjens, A. V.; de Bruin, J. G. *J. Polym. Sci., Part B: Polym. Phys.* **1992**, *30*, 83−90.
(81) Koros, W. J.; Fleming, G. K. *J. Membr. Sci.* **1993**, *83*, 1−80.
(82) Koros, W. J.; Hellums, M. W. In *Encyclopedia of Polymer Science and Engineering*, 2nd ed.; Mark, H. F., Bikales, N. M., Overberger, C. G., Mendes, G., Eds.; Wiley-Interscience: New York, 1989; Suppl. Vol.
(83) Koros, W. J.; Chan, A. H.; Paul, D. R. *J. Membr. Sci.* **1997**, *2*, 165.
(84) Costello L. M.; Koros, W. J. *Ind. Eng. Chem. Res.* **1992**, *31*, 2708.
(85) Hellums, M. W.; Koros, W. J.; Husk, G. R.; Paul, D. R. *J. Membr. Sci.* **1989**, *46*, 93.
(86) Hofman, D.; Ulbrich, J.; Fritsch, D.; Paul, D. *Polymer* **1996**, *37*, 4773−4785.
(87) Kovacs, A. J.; Aklonis, J. J.; Hutchinson, J. M.; Ramos, A. R. *J. Polym. Sci., Polym. Phys. Ed.* **1979**, *17*, 1097−1162.
(88) Tool, A. Q. *J. Am. Ceram. Soc.* **1948**, *31*, 177−186.
(89) Kovacs, A. J. In *Structure and Mobility in Molecular and Atomic Glasses*, O'Reilly, J. M., Goldstein, M., Eds.; *Ann. N.Y. Acad. Sci.* **1981**, *371*, 38−66.
(90) Heymans, N.; Dequenne, B. *Polymer* **2001**, *42*, 5337−5342.
(91) Murayama, T. *Dynamic Mechanical Analysis of Polymeric Materials*; Elsevier: New York, 1978.
(92) Turi, E. A. *Thermal Characterization of Polymeric Materials*, 2nd ed.; Academic Press: New York, 1997; Vol. 1.
(93) Fox, T. G.; Flory, P. J. *J. Am. Chem. Soc.* **1948**, *70*, 2384.
(94) Fox, T. G.; Flory, P. J. *J. Appl. Phys.* **1950**, *21*, 581.
(95) Jean, Y. C.; Rhee, Y.; Lou, Y.; Shelby, D.; Wilkes, G. L. *J. Polym. Sci., Part B: Polym. Phys.* **1996**, *34*, 2979−2985.
(96) Shelby, M. D.; Wilkes, G. L. *J. Polym. Sci., Part B: Polym. Phys.* **1998**, *36*, 2111.
(97) Shelby, M. D.; Wilkes, G. L. *Polymer* **1998**, *39*, 6767−6779.
(98) Schmittmann, B.; Zia, R. K. P.; Marand, E., to be published.
(99) Kirchheim, R. *Prog. Mater. Sci.* **1988**, *32*, 262.
(100) Pönitsch, M.; Gotthardt, P.; Gruger, A.; Brion, H. G.; Kirchheim, R. *J. Polym. Sci., Polym. Phys.* **1997**, *35*, 2397.

MA021720O